IV Escola de Primavera de Transição e Turbulência
Universidade Federal do Rio Grande do Sul
Pontifícia Universidade Católica do Rio Grande do Sul
Porto Alegre, RS, 27 de setembro a 1° de outubro de 2004

COMPARISON AMONG RANS TURBULENCE MODELS

Francisco José de Souza
Laboratory of Heat and Mass Transfer and Fluid Dynamics – LTCM
School of Mechanical Engineering – Bloco 1M
Federal University of Uberlândia
Av. João Naves de Ávila, 2121
Uberlândia – MG- Brazil
e-mail: fjsouza@mecanica.ufu.br

Aristeu da Silveira Neto
Laboratory of Heat and Mass Transfer and Fluid Dynamics – LTCM
School of Mechanical Engineering – Bloco 1M
Federal University of Uberlândia
Av. João Naves de Ávila, 2121
Uberlândia – MG- Brazil
e-mail: aristeus@mecanica.ufu.br

Abstract. *The purpose of this paper is to compare the performance of three RANS turbulence models, namely the realizable κ-ε, the Spalart-Allmaras and the v^2-f κ-ε models, in the computation of the flow over a backward facing step. These models were implemented in a 2-D, finite-volume code based on the SIMPLE algorithm. It was possible to conclude that the recirculation region in the backward facing step case is overpredicted by the Spalart-Allmaras model, whereas both the realizable and the v^2-f κ-ε models generally provide good agreement with the experimental data.*

Keywords*. RANS models performance, backward facing step, v^2-f κ-ε model.*

1. Introduction

The choice of the appropriate turbulence model is a key element in a sucessful flow prediction. Development of turbulence models has increased in the last decade due to technological requirements. Nevertheless, the lack of information about their performance has disencouraged usage of these models under different flow conditions. Thus, validation and testing of turbulence models are needed to understand their capabilities and limitations (Bardina et al, 1997).

In this paper, three advanced Reynolds-averaged Navier-Stokes (RANS) turbulence models were selected: the realizable κ-ε, the Spalart-Allmaras and the v^2-f κ-ε models. These models are claimed to improve the ability of the so-called more classical models, e.g. standard κ-ε model, to predict near-wall behavior and reverse flow, for instance.

This initial study employs one classical test cases, for which the results of other turbulence models are known: the backward facing step. This flow represents a challenge for most turbulence models, since separation, reattachment and redeveloping flow are some of the features present in this test case. Essentially, the mean velocity profiles are compared with the results from the simulatons.

These turbulence models were implemented in the CAFFA code (Ferziger and Peric, 1999). This is a 2D, finite-volume, incompressible code with boundary-fitted coordinates and the collocated arrangement. The SIMPLE algorithm was used for coupling pressure and velocity.

2. Formulation

2.1. Baseline code

The baseline code solves the incompressible 2D Navier-Stokes equations in a conservative finite-volume formulation by means of the SIMPLE algorithm. The second-order centered scheme was used to discretize the advective e diffusive terms. Also, the collocated arrangement with the Rhie-Chow interpolation was used to compute velocities at the cell faces. Only steady-state computations were considered in this work, though the code allows time-dependent calculations.

2.2. Spalart-Allmaras model

The Spalart-Allmaras model (Spalart and Allmaras, 1992 and Wilcox, 1993) is a relatively recent eddy viscosity model based on a transport equation for the turbulent viscosity. This model was inspired from an earlier model developed by Baldwin and Barth (1990). Its formulation and coefficients were defined using dimensional analysis, Galilean invariance, and selected empirical results.

The aim of this model is to improve the predictions obtained with algebraic mixing-length models to develop a local model for complex flows, and to provide a simpler alternative to two-equation turbulence models.

This model uses distance to the nearest wall in its formulation, and provides smooth laminar-turbulent capabilities, provided that the location of the start of the transition is given. It does not require as fine a grid resolution in wall-bounded flows as two-equation turbulence models, and it shows good convergence in simpler flows.

This model does not give good predictions in jet flows, but gives reasonably good predictions of 2d mixing layers, wake flows, and flat-plate boundary layers and shows improvements in the predictions of flows with adverse pressure gradients compared with the κ-ε and κ-ω models.

The eddy viscosity function is defined in terms of an eddy viscosity variable, $\tilde{\nu}$, and a wall function, f_{v1}, as follows:

$$\nu_t = \tilde{\nu} f_{v1} \tag{1}$$

The convective transport equation of the eddy viscosity is modeled as:

$$\frac{\partial \rho \tilde{\nu}}{\partial t} + \frac{\partial \left(\rho u_j \tilde{\nu}\right)}{\partial x_j} = c_{b1} \rho \tilde{S} \tilde{\nu} + \frac{1}{\sigma} \frac{\partial}{\partial x_k} \left[\rho \left(\nu + \tilde{\nu}\right) \frac{\partial \tilde{\nu}}{\partial x_k} \right] + \frac{c_{b2}}{\sigma} \rho \frac{\partial \tilde{\nu}}{\partial x_k} \frac{\partial \tilde{\nu}}{\partial x_k} - c_{w1} f_w \rho \left(\frac{\tilde{\nu}}{d}\right)^2 \tag{2}$$

where the right-hand-side terms represent turbulence eddy viscosity production, conservative diffusion, nonconservative diffusion, near-wall turbulence destruction, transition damping of the production. The transition terms have been neglected in this work. ρ is the fluid density and d is the distance to the closest wall.

The model constants and auxiliary functions are defined in terms of the basic model for free-shear flows, the wall model for boundary layers, the viscous model for integration to the wall.

The basic model constants for free-shear flows to control the production and diffusion of turbulent eddy viscosity are:

$$c_{b1} = 0.1355 \qquad c_{b2} = 0.622 \qquad \sigma = 2/3 \qquad k = 0.41$$

where k is the von Karman constant.

The additional model constants and auxiliary functions for the destruction of turbulent eddy viscosity in the boundary layer zone are:

$$c_{w1} = c_{b1}/k^2 + \left(1 + c_{b2}\right)/\sigma \qquad r = \frac{\tilde{\nu}}{\tilde{S} k^2 d^2} \qquad c_{w2} = 0.3 \qquad c_{w3} = 2 \qquad g = r + c_{w2}\left(r^6 - r\right) \qquad f_w = g\left(\frac{1 + c_{w3}^6}{g^6 + c_{w3}^6}\right)^{1/6}$$

Modeling functions and constants for the near wall flow regions are given by:

$$\tilde{S} = S + \frac{\tilde{\nu}}{(kd)^2} f_{v2} \qquad S = \sqrt{2 S_{ij} S_{ij}} \qquad S_{ij} = \frac{1}{2}\left(\frac{\partial u_i}{\partial x_j} + \frac{\partial u_j}{\partial x_i}\right)$$

$$\chi = \frac{\tilde{\nu}}{\nu} \qquad f_{v1} = \frac{\chi^3}{\chi^3 + c_{v1}^3} \qquad f_{v2} = 1 - \frac{\chi}{1 + \chi f_{v1}} \qquad c_{v1} = 7.1$$

Boundary conditions for this model are: $\tilde{\nu} = 0$ at walls and inlets, and zero gradient for outlet and symmetry boundaries.

2.3. Realizable κ-ε model

The purpose of this model, which was proposed by Shih et al (1994), is to provide new formulations for the dissipation rate and eddy viscosity in order to improve the performance of the standard κ-ε model. The new model dissipation rate equation is based on the dynamic equation for the fluctuation vorticity. The new formulation for the eddy viscosity contains the effect of mean rotation on the turbulent stresses ensures the square of the normal stresses are positive. Results for rotating homogeneous shear flows, free shear flows, channel flows with and without pressure gradients and backward facing steps show that this model performs better than the standard κ-ε in almost all cases.

The eddy viscosity for this model is obtained from:

$$\mu_t = \min\left\{ C_\mu f_\mu \rho \frac{\kappa^2}{\varepsilon}, \frac{2\rho\kappa}{3S} \right\}, \tag{3}$$

where $S = \sqrt{2S_{ij}S_{ij}}$ is the strain magnitude and f_μ is a low-Reynolds number function, designed to account for viscous and inviscid damping turbulent fluctuations in the proximity of solid surfaces:

$$f_\mu = \frac{1-e^{-0.01\,Re_t}}{1-e^{-\sqrt{Re_t}}}\max\left\{1,\sqrt{\frac{2}{Re_t}}\right\}. \tag{4}$$

The realizable κ-ε model consists of the following transport equations for κ and ε:

$$\frac{\partial(\rho\kappa)}{\partial t} = P - \rho\varepsilon - \frac{\partial(\rho u_j \kappa)}{\partial x_j} + \frac{\partial}{\partial x_i}\left[\left(\mu_m + \frac{\mu_t}{\sigma_\kappa}\right)\frac{\partial\kappa}{\partial x_i}\right], \tag{5}$$

$$\frac{\partial(\rho\varepsilon)}{\partial t} = \frac{(C_{\varepsilon 1}P - C_{\varepsilon 2}\rho\varepsilon + E)}{T_t} - \frac{\partial(\rho u_j \varepsilon)}{\partial x_j} + \frac{\partial}{\partial x_i}\left[\left(\mu_m + \frac{\mu_t}{\sigma_\varepsilon}\right)\frac{\partial\varepsilon}{\partial x_i}\right], \tag{6}$$

where P is the production term, given by:

$$P = \mu_t\left(\frac{\partial u_i}{\partial x_j} + \frac{\partial u_j}{\partial x_i}\right)^2, \tag{7}$$

and the additional term E in the dissipation-rate equation is designed to improve the model response to adverse pressure-gradient flows is:

$$E = 0.3\rho\sqrt{\varepsilon T_t}\Psi\max\left\{\kappa^{1/2},(\nu\varepsilon)^{1/4}\right\}, \tag{8}$$

$$\Psi = \max\left\{\frac{\partial\kappa}{\partial x_j}\frac{\partial(\kappa/\varepsilon)}{\partial x_j}\right\}. \tag{9}$$

T_t is a realizable estimate of the turbulence timescale:

$$T_t = \frac{\kappa}{\varepsilon}\max\left\{1,\sqrt{\frac{2}{Re_t}}\right\}, \tag{10}$$

and Re_t is the turbulence Reynolds number, $Re_t = (\rho\kappa^2)/(\mu\varepsilon)$.

At wall boundary conditions κ is set to zero and ε has a zero normal gradient. At symmetry and outlet boundaries, zero gradients are applied to both variables. Inlet boundaries will be discussed further.

2.4. v^2-f κ-ε model

The v^2-f model, based on v^2 κ-ε Durbin's model (Durbin, 1995), is an alternative to eddy-viscosity models and the RSM (Reynolds Stress Model). The v^2-f κ-ε model is similar to the standard v^2-κ-ε model, but incorporates near-wall turbulence anisotropy and non-local pressure-strain effects (Fluent manual, 2003).

The distinguishing feature of the v^2f model is the use of the velocity scale, v^2, instead of the turbulence kinetic energy, κ, for evaluating the eddy viscosity. v^2, which can be thought of as the velocity fluctuation normal to he streamlines, has shown to provide the right scaling in representing the damping of turbulent transport close to the wall,a feature that κ does not provide.

It is a general low-Reynolds-number turbulence model that is valid all the way up to solid walls, and therefore does not need to make use of wall functions. Although the model was originally developed for attached or mildly separated boundary layers, it is also claimed to accurately simulate flows dominated by separation.

The eddy viscosity for this model is obtained from:

$$\mu_t = \rho C_\mu v^2 T, \tag{11}$$

The turbulence kinetic energy, κ, its rate of dissipation, ε, the velocity variance scale, v^2, and the elliptic relaxation function, f, are obtained from the following transport equations:

$$\frac{\partial(\rho\kappa)}{\partial t}+\frac{\partial(\rho\kappa u_i)}{\partial x_i}=P-\rho\varepsilon+\frac{\partial}{\partial x_j}\left[\left(\mu+\frac{\mu_t}{\sigma_k}\right)\frac{\partial\kappa}{\partial x_j}\right], \tag{12}$$

$$\frac{\partial(\rho\varepsilon)}{\partial t}+\frac{\partial(\rho\varepsilon u_i)}{\partial x_i}=\frac{C'_{\varepsilon 1}P-C_{\varepsilon 2}\rho\varepsilon}{T}+\frac{\partial}{\partial x_j}\left[\left(\mu+\frac{\mu_t}{\sigma_\varepsilon}\right)\frac{\partial\varepsilon}{\partial x_j}\right], \tag{13}$$

$$\frac{\partial(\rho v^2)}{\partial t}+\frac{\partial(\rho v^2 u_i)}{\partial x_i}=\rho\kappa f-6\rho v^2\frac{\varepsilon}{\kappa}+\frac{\partial}{\partial x_j}\left[\left(\mu+\frac{\mu_t}{\sigma_k}\right)\frac{\partial v^2}{\partial x_j}\right], \tag{14}$$

$$f-L^2\frac{\partial^2 f}{\partial x_j^2}=(C_1-1)\frac{\frac{2}{3}-\frac{v^2}{\kappa}}{T}+C_2\frac{P}{\rho\kappa}+\frac{\frac{5v^2}{\kappa}}{T}, \tag{15}$$

where P is as given by Eq.(7) and the turbulent time scale T and length scale L are defined by:

$$T'=\max\left[\frac{\kappa}{\varepsilon},6\sqrt{\frac{\nu}{\varepsilon}}\right], \tag{16}$$

$$T=\min\left[T',\frac{0.6}{\sqrt{3}}\frac{\kappa}{v^2 C_\mu S}\right], \tag{17}$$

$$L'=\min\left[\frac{\kappa^{\frac{3}{2}}}{\varepsilon},\frac{1}{\sqrt{3}}\frac{\kappa^{\frac{3}{2}}}{v^2 C_\mu S}\right], \tag{18}$$

$$L=C_L\max\left[L',C_\eta\left(\frac{\nu^3}{\varepsilon}\right)^{\frac{1}{4}}\right]. \tag{19}$$

The variable f is the solution to the elliptic relaxation equation (Eq. 5). Here, the v^2-f model uses an elliptic operator to compute a term analogous to the pressure-strain correlation of the RSM. Ellipticity is characterized by a modified Helmholtz operator, which introduces wall effects via a linear differential equation.

The model constants have the following default values (Behnia et al, 1999 and Parneix et al, 1998):

$C_1=1.4$, $C_2=0.3$, $C_{\varepsilon 1}=1.4$, $C_{\varepsilon 2}=1.9$, $C_\eta=70$,

$C_\mu=0.22$, $C_L=0.23$, $\sigma_k=1$, $\sigma_\varepsilon=1.3$, $C'_{\varepsilon 1}=C_{\varepsilon 1}\left(1+0.045\sqrt{\kappa/v^2}\right)$

The boundary conditions for κ and ε are the same as those for the realizable κ-ε. The boundary conditions for v^2 are the same as those for κ, except at the inlet, where v^2 is set to 2/3 of κ. For the auxiliary variable f, at walls f = 0 and zero gradients are applied to all the other boundaries.

3. Implementation of the Turbulence Models

All the turbulent variables were treated as scalars in the code, their implementation being straightforward. For the discretization of the convective and diffusive terms of all the models, the first-order upwind and the second-order centered schemes were used, respectively. The three-time-level scheme is used for the transient term, though only steady-state computations were run.

4. Backward Facing Step Configuration

The backward-facing step is a popular choice for computational fluid dynamicists because it is a combination of simple geometry and complex flow. Separation, reattachment and re-developing flow are some of the features present in this test-case. The incompressible flow downstream of the step with an expansion ratio of 1.25 is modeled. The experiments were accomplished by Vogel and Eaton (1984). The geometrical configuration for this test case is shown in Figure 1. The outlet boundary is located approximately 40 H downstream of the step. The Reynolds number is based on the freestream inlet speed, u_∞, the step height, H, and the viscosity of the fluid, ν:

$$\mathrm{Re} = \frac{u_\infty H}{\nu}, \tag{20}$$

is 28000. In the experiment, the inlet profile evolved in a rectangular duct. Thus, the boundary layer profile at the inlet was imposed according to the experimental values available (Vogel and Eaton, 1984).

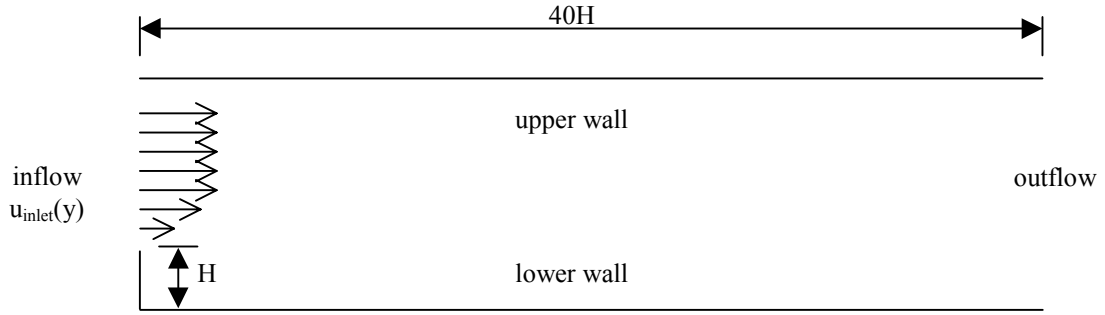

Figure 1: Computational domain for the turbulent flow over a backward-facing step.

5. Results

The computations whose results are shown were performed on a 120 x 120 grid, with substantial refinement near the step. In order to ensure that these results are grid-independent, the computations were run on a 80 x 80 and on a 160 x 160 grid, and identical results were obtained.

For both the realizable e v^2f κ-ε models, the turbulence inlet conditions were specified as follows: κ was computed assuming 5% turbulence intensity (I) in the inlet streamwise velocity (u_{inlet}):

$$\kappa = 1.5(\mathrm{I}u_{inlet})^2. \tag{21}$$

To obtain the dissipation rate at the inlet, the following relation was employed:

$$\varepsilon = C_\mu^{0.75}\left(\frac{\kappa^{1.5}}{\ell}\right), \tag{22}$$

where ℓ is the length scale in the boundary layer, which is assumed to be 0.085δ, δ being the boundary layer thickness.

Convergence with the v^2f was obtained only when the computation was initialized with the converged solution of the realizable κ-ε model. In this case, v^2 and f were set to 2/3 of κ and 1, respectively, over the computational domain.

Figures 2(a) to 2(j) compare the mean streamwise velocity component at different stations downstream of the step. Generally speaking, it can be seen that the results of all models reasonably agree with the experimental data. The reverse flow region down the step was captured by the three models. Right after the step, it can be seen that the v^2f model seems to provide better agreement with experiments than the other two models, though the mean flow was equally well predicted by all models. The Spalart-Allmaras model tended to overpredict the recirculation velocities as well as the recirculation length, as can be seen in Figs. 2(b) to 2(e). This might have been due to inlet boundary conditions, but sensitivity studies showed that the Spalart-Allmaras model results were independent of turbulence inlet conditions as long as $\tilde{\nu}$ was kept below ten times the molecular viscosity.

The realizable κ-ε model appears to give the best overall results, providing accurate predictions for the reverse-flow regions and the redeveloping flow. This was somehow expected since the additional term E (Eq. 8)in the dissipation rate equation is designed to improve the model response to adverse pressure-gradient flows.

From a certain station on (x/H=12.2), the plots show that the results of the realizable and v^2-f κ-ε models overlap. In fact, the modifications these models bring with regard to the standard κ-ε are related to recirculation flow regions. Therefore, it is not surprising to obtain the same behavior in the redeveloped flow. The Spalart-Allmaras model underpredicts the near-wall velocities, although in the mean flow it attempts to approach the experimental results better than the κ-ε models.

Table 1 displays the reattachment length predicted by the models. Since the experimental value lies between x/H=6 and x/H=7, it is possible to conclude that the Spalart-Allmaras model did not provide an accurate estimate for the reattachment length.

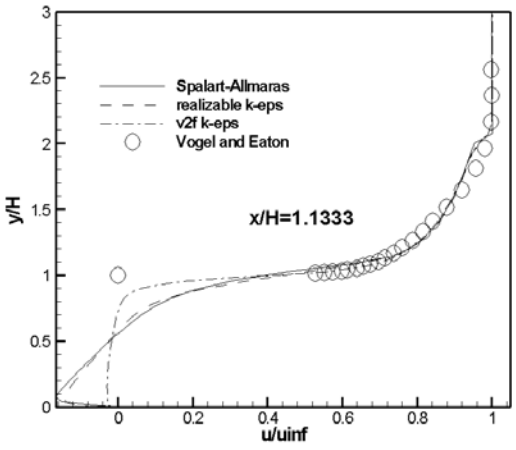

2(a)

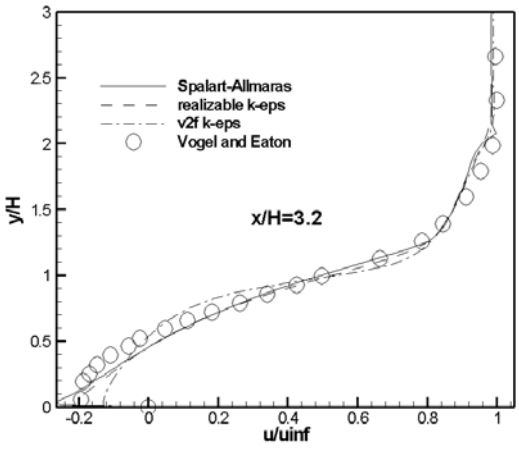

2(b)

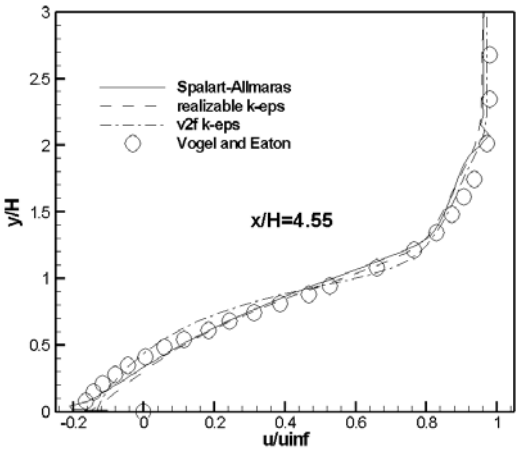

2(c)

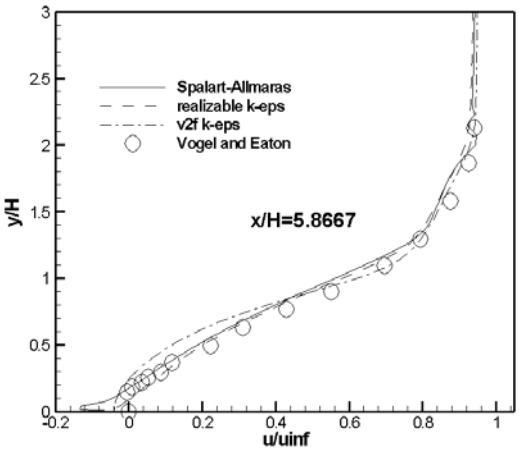

2(d)

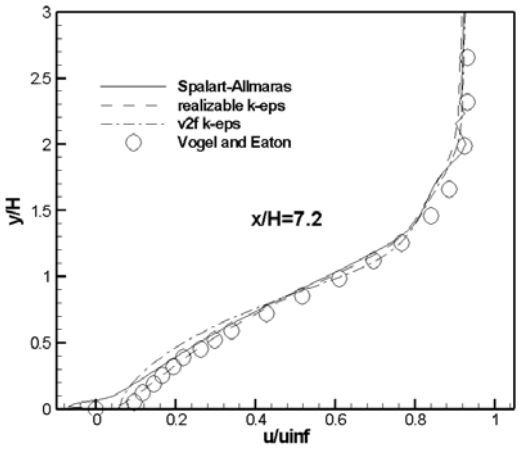

2(e)

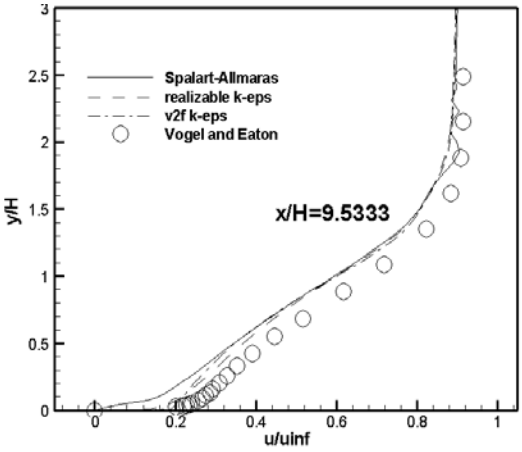

2(f)

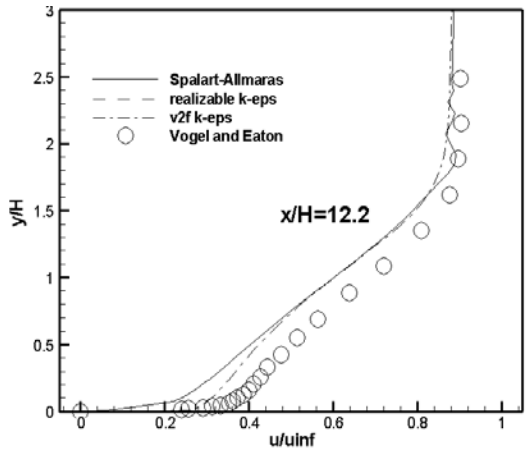

2(g)

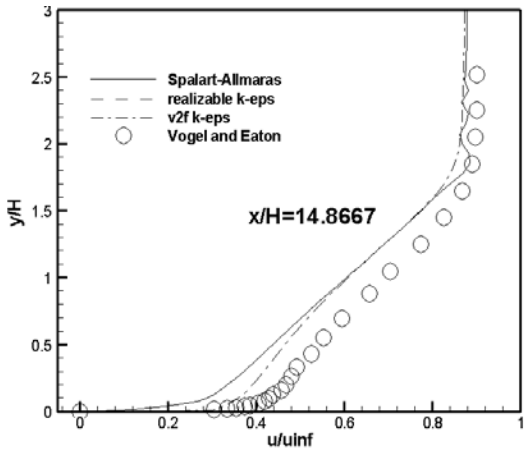

2(h)

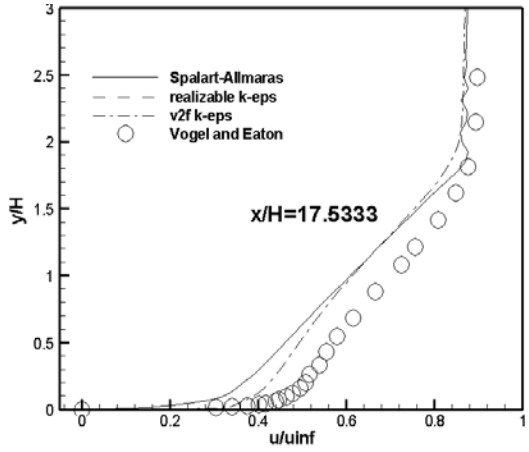

2(i)

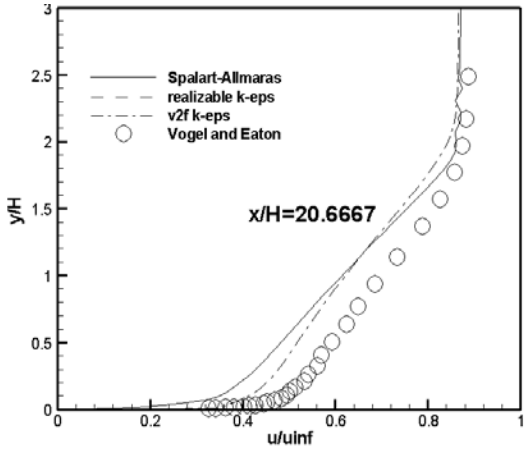

2(j)

Figure 2. Streamwise velocity predictions by the three models and experimental data at different horizontal stations.

Table 1. Backward-facing step reattachment length predictions.

Model	Reattachment length x/H
Spalart-Allmaras	8.5
Realizable κ-ε	6.5
v^2-f κ-ε	6.3

Another interesting discrepancy among these models is in the region in the corner of the step. Figures 3, 4 and 5 show the streamlines in that section for the three models. It can be clearly seen that both the realizable κ-ε and the Spalart-Allmaras models capture a small counterclockwise recirculation eddy right in the corner of the step, while the v^2f smoothes it. This eddy is known to be present above a certain Reynolds number and even though the profiles computed with the v^2f agree better with the experiments at the first station, as shown in Fig. 2(a), this model was not accurate enough to predict the recirculation phenomena in this region. Also, the center of the largest eddy is located considerably ahead of those computed with the realizable and Spalart-Allmaras models.

6. Conclusions

Three RANS models, namely the Spalart-Allmaras, the realizable κ-ε and the v^2-f κ-ε models, were tested in a backward-facing step flow with regard to the their ability to predict mean velocities. The Spalart-Allmaras model was seen to overpredict the recirculation magnitude and reattachment length, while both κ-ε models results agreed well with the experimental data. The v^2f model failed to predict the existence of a small eddy in the corner of the step and the predictions of the other two models agreed with each other with regard to the position of this eddy. The best overall model for the particular test case is judged to be the realizable κ-ε model, whose results agree with experiments over separated, reattached and redeveloped flow regions.

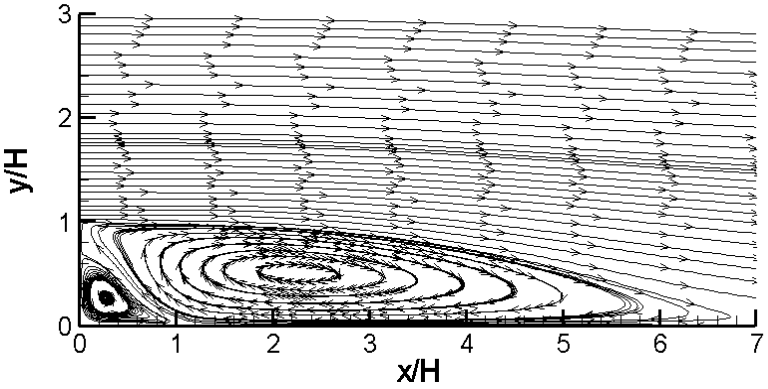

Figure 3. Recirculation eddies at the edge of the step predicted by the Spalart-Allmaras model.

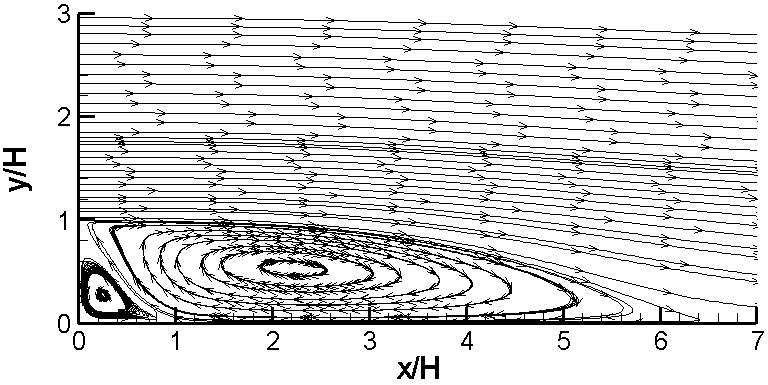

Figure 4. Recirculation eddies at the edge of the step predicted by the realizable κ-ε model.

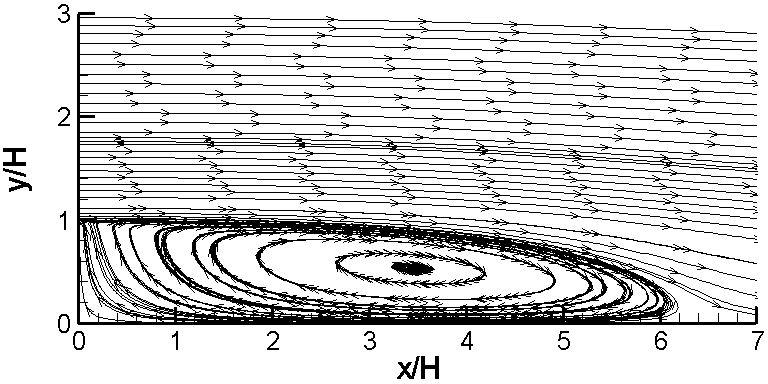

Figure 5. Recirculation eddies at the edge of the step predicted by the v^2-f κ-ε model.

7. References

Baldwin, B. S. and Barth, T. J., 1990, "A One-Equation Turbulence Transport Model for High Reynolds Number Wall-Bounded Flows". NASA TM-102847.

Bardina, J. E., Huang, P. G. and Coakley, T. J., 1997, "Turbulence Modeling Validation, Testing and Development", NASA TM 110446.

Behnia, M, Parneix, S., Shabany, Y. and Durbin, P. A., 1999, "Numerical Study of Turbulent Heat Transfer in Confined and Unconfined Impinging Jets", International Journal of Heat and Fluid Flow, Vol. 20, pp.1-9.

Durbin, P. A., 1995, "Separated Flow Computations with the κ-ε-v^2 Model". AIAA Journal, 33(4), pp. 659-664.

Ferziger, J. and Peric, M., 1999, "Computational Methods for Fluid Dynamics", Spring-Verlag, 390 p.

Parneix, S., Durbin, P. A. and Behnia, M., 1998, "Computation of a 3D Turbulent Boundary Layer Using the v^2-f Model". Flow Turbulence and Combustion, Vol. 10, pp. 19-46.

Shih, T. H., Liou, W. W., Shabbir, A., Yang, Z. and Zhu, J. 1994, "A New Eddy Viscosity Model for High Reynolds Number Turbulent Flows – Model Development and Validation". NASA TM 106721.

Spalart, P. R. and Allmaras, S. R., 1992, “A One-Equation Turbulence Model for Aerodynamic Flows”. AIAA Paper 92-0439

Vogel, J. C. and Eaton, J. K., 1984, “Heat Transfer and Fluid Mechanica Measurements in the Turbulent Reattaching Flow Behind a Backward-Facing Step”, Report MD-44, Thermociences Division, Dept. of Mechanical Engineering, Stanford University.

Wilcox, D. C., 1993, “Turbulence Modeling for CFD”. DCW industries, Inc., 5354 Palm Drive, La Cañada, Calif.

8. Copyright Notice